

# Biomechanical Evaluation of an Interfacet Joint Decompression and Stabilization System

**Jeremi M. Leasure<sup>1</sup>**

The Taylor Collaboration,  
St. Mary's Medical Center,  
San Francisco, CA 94117;  
San Francisco Orthopaedic Residency Program,  
San Francisco, CA 94117  
e-mail: jleasure@taylorcollaboration.org

**Jenni Buckley**

The Taylor Collaboration,  
St. Mary's Medical Center,  
San Francisco, CA 94117;  
University of Delaware Department of  
Mechanical Engineering,  
Newark, DE 19716

*A majority of the middle-aged population exhibit cervical spondylosis that may require decompression and fusion of the affected level. Minimally invasive cervical fusion is an attractive option for decreasing operative time, morbidity, and mortality rates. A novel interfacet joint spacer (DTRAX facet screw system, Providence Medical) promises minimally invasive deployment resulting in decompression of the neuroforamen and interfacet fusion. The present study investigates the effectiveness of the device in minimizing intervertebral motion to promote fusion, decompression of the nerve root during bending activity, and performance of the implant to adhere to anatomy during repeated bending loads. We observed flexion, extension, lateral bending, and axial rotation resonant overshoot mode (ROM) in cadaver models of c-spine treated with the interfacet joint spacer (FJ spacer) as stand-alone and supplementing anterior plating. The FJ spacer was deployed bilaterally at single levels. Specimens were placed at the limit of ROM in flexion, extension, axial bending, and lateral bending. 3D images of the foramen were taken and postprocessed to quantify changes in foraminal area. Stand-alone spacer specimens were subjected to 30,000 cycles at 2 Hz of nonsimultaneous flexion-extension and lateral bending under compressive load and X-ray imaged at regular cycle intervals for quantitative measurements of device loosening. The stand-alone FJ spacer increased specimen stiffness in all directions except extension. 86% of all deployments resulted in some level of foraminal distraction. The rate of effective distraction was maintained in flexed, extended, and axially rotated postures. Two specimens demonstrated no detectable implant loosening (<0.25 mm). Three showed unilateral subclinical loosening (0.4 mm maximum), and one had subclinical loosening bilaterally (0.5 mm maximum). Results of our study are comparable to previous investigations into the stiffness of other stand-alone minimally invasive technologies. The FJ spacer system effectively increased stiffness of the affected level comparable to predicate systems. Results of this study indicate the FJ spacer increases foraminal area in the cervical spine, and decompression is maintained during bending activities. Clinical studies will be necessary to determine whether the magnitude of decompression observed in this cadaveric study will effectively treat cervical radiculopathy; however, results of this study, taken in context of successful decompression treatments in the lumbar spine, are promising for the continued development of this product. Results of this biomechanical study are encouraging for the continued investigation of this device in animal and clinical trials, as they suggest the device is well fixated and mechanically competent. [DOI: 10.1115/1.4026363]*

*Keywords: cervical, fusion, foraminal, decompression, intervertebral*

## Introduction

Over 50% of the middle-aged population exhibits radiological or pathological evidence of cervical spondylosis [1–3]. This condition is often asymptomatic; however, in up to 15% of these cases the condition progresses to root or cord compression [4,5]. Nerve root compression is linked to cervical radiculopathy and is most commonly caused by narrowing of the foraminal space secondary to spondylarthrosis and herniated disks [6–8].

The aim for all surgical treatments of this indication is fusion and nerve root decompression of the affected level [9]. One treatment for this indication is open posterior approach direct foraminotomy. An open anterior approach may also be utilized with a combined discectomy and allograft strut fusion. Both approaches focus on fusion the affected level and both are performed via open

surgery. The ability to achieve rigid fixation for short-segment cervical fusions through a stand-alone minimally invasive surgical (MIS) approach is an attractive option, as it translates into decreased perioperative time and patient morbidity.

Percutaneous transfacet screws have been utilized as a supplemental MIS technique in combination with anterior decompression and fusion [10–12]. Future directions for this posterior approach technique include utilization as a stand-alone procedure [13]. While percutaneous transfacet screws may be an option for stand-alone fusion, the technique may not address the need for direct decompression of the neuroforaminal space. The transfacet technique has been compared to traditional lateral mass/pedicle screws and rods in the biomechanics literature [10–12]; however, previous investigations have only reported range of motion stabilization without an evaluation of the neuroforaminal decompression or performance of the device under repeated physiological loading.

Recently, a novel MIS device has been developed to treat cervical foraminal stenosis. The interfacet joint spacer (DTRAX, Providence Medical Technology) consists of a screw and washer that

<sup>1</sup>Corresponding author.

Manuscript received April 2, 2013; final manuscript received December 17, 2013; accepted manuscript posted December 30, 2013; published online May 22, 2014. Assoc. Editor: Brian D. Stemper.

distracts and immobilizes the cervical facet for root decompression and fusion. The device is deployed percutaneously between the facet surfaces. Decompression and fusion of the level is achieved by advancing the screw within the nut, thus, distracting the facet increasing foraminal area and stabilizing the relative motion between the vertebral bodies. The ability of the interfacet joint spacer (FJ spacer) to effectively decompress the cervical foramen has yet to be proven. The efficacy of this device will depend on many factors, including decreased range of motion (ROM) across the fusion site, distraction of the affected foramen, and maintenance of its deployment position during repeated bending motion and loading. Ideally the device should perform favorably during each scenario as a stand-alone fixation device but potentially also as part of an anterior-posterior fixation construct.

The goal of our study was to evaluate the biomechanical efficacy of the FJ spacer system in vitro. We aimed to evaluate three aspects of the devices performance, including acute stabilization, neuroforaminal distraction, and migration of the implant over time due to repeated loading. The specific aims and hypotheses of our study were:

- (1) Quantify the amount of stability introduced by the deployment of the device as a stand-alone procedure and combined with anterior cervical plating in a cadaver model. We hypothesized range of motion would be significantly limited as a consequence of stand-alone device deployment and the addition of the anterior plate would not significantly increase stiffness.
- (2) Evaluate the device's ability to effectively decompress the neuroforaminal space in a cadaver model. We hypothesized the stand-alone device would significantly increase foraminal area throughout bending motion.
- (3) Evaluate the fatigue performance of this device deployed in a stand-alone configuration. We performed this evaluation in a cadaver model, measuring the amount of device migration while implanted and tested in a flexion/extension and lateral bending cyclic loading model. We hypothesized the device would not significantly change its position/migrate over time under repeated loading.

### Methods for Multidirectional Bending Stability

**Specimen Preparation.** Intact, fresh-frozen cervical spines (C2-T2, N-5, three male, two female, ages 68 to 95) were procured and examined physically and radiographically for pathological conditions or prior surgery to that region. Specimens were cleaned of skin and paravertebral muscle and potted to midaxial height at the C3 and T1 levels using quick-set resin (SmoothCast). Multiaxial range-of-motion tests were conducted for every specimen in its intact state and following three different surgical procedures. The treatment level of interest was C4/5, and the procedures were performed in the following sequence:

- (1) Destabilization: Early stage cervical stenosis was modeled by destabilizing C4/5 via nucleotomy. The technique was as follows. An 18 gauge needle was inserted anteriorly into the disk space. The needle was removed and either a small curette or pituitary (4 mm maximum diameter) was used to remove nucleus material. A blunt tipped, curved dental pick was inserted periodically to confirm the integrity of the inner annular wall. Nucleus material was removed. All procedures were performed following the clinical guidelines for cervical microdiscectomy technique outlined by Ahn et al. [14].
- (2) Stand-alone device. The FJ spacer was deployed bilaterally and tested as a stand-alone construct.
- (3) Device + anterior plate. A single-level anterior plate (Medtronic, Atlantis) at C4/5 was supplemented to the bilateral FJ spacer deployment.

**Mechanical Testing.** A standard, moment-controlled pure moment testing protocol [15,16] was used to conduct multi-axial

ROM tests on the cervical spines. Specimens were attached to a cable-driven pure moment testing apparatus on a uniaxial test frame (MTS 858 Bionix) and sequentially tested in each of six loading directions: flexion, extension, right and left lateral bending, and right and left axial rotation. The order of testing was randomized to minimize bias. In each loading mode, specimens were tested to a maximum of 1.5 Nm under moment-controlled loading conditions. A stepwise loading sequence was applied, with 0.25 Nm loading increments every 45 s to allow for specimen settling. Specimens were subjected to three loading cycles with data collected on the final cycle. Moment was calculated in real-time during testing using an in-line load cell to measure cable tension, and relative vertebral motion was monitored using a 3D motion tracking camera system (Optotrak 3020) with customized kinematic software for spinal applications. Motion tracking rigid body markers were attached at the C4 and C5 vertebral levels.

**Outcome Measures and Statistical Analysis.** The primary outcome measures from biomechanical testing were total C4–C5 relative motion (deg) and ROM stiffness (Nm/deg) in the applied loading direction, e.g., flexion angle under flexion loading. Stiffness was calculated as the loading moment divided by the total number of degrees of relative motion. Stiffness values were further processed for each treatment group as percent higher or lower than intact values, calculated as the stiffness of the treatment group divided by the stiffness of the intact specimen. A repeated measures analysis of variance (ANOVA) with post hoc adjustment for individual comparisons were used to evaluate statistically significant differences in the outcome measures with  $\alpha$  equal to 0.05.

### Methods for Foraminal Distraction

**Specimen Preparation.** Intact head and neck specimens ( $N=2$ , cranium-T2, ages 71 and 65, one male and one female) were acquired for this study. Planar X-ray images were taken prior to deployment of the device to exclude specimens with pathological conditions, including pre-existing vertebral fractures, severe osteophyte formation, sagittal plane deformity, or Paget's disease. The device was inserted bilaterally at C4–C5, C5–C6, and C6–C7 levels. Insertion was performed with a c-arm available to facilitate and document device positioning. Foramen specimens were placed in the prone position on a cantilevered, c-arm compatible table. A Mayfield halo was rigidly attached to the cranium, and the halo was attached to wooden guide rods attached to the surgical table as shown in Fig. 1.



**Fig. 1** A test specimen in the custom-designed jig used for positioning during radiographic examination of foraminal area specimens. This specimen is shown positioned in left axial rotation. The c-arm was positioned to encircle the specimen during its 3D data capture.

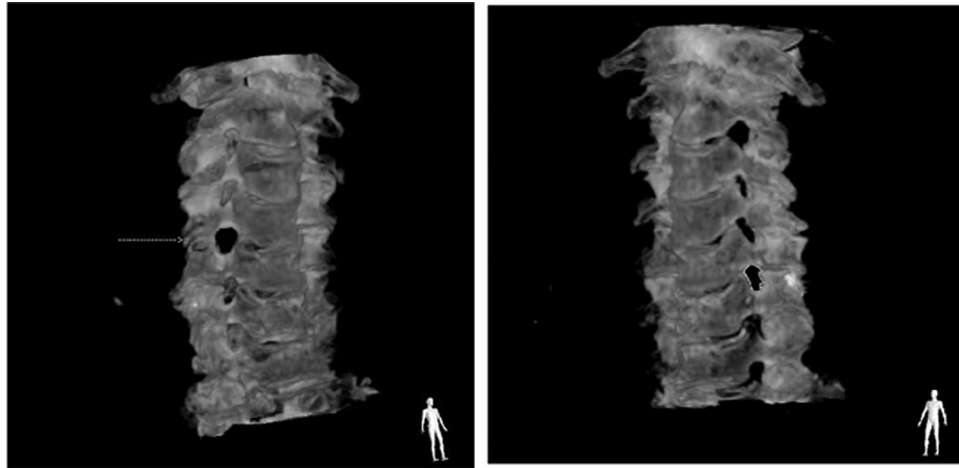


**Fig. 2** (left) A rendered image from the 3D c-arm system. The rendering is positioned for measurement of right C4/5 foraminal geometry. (right) Foraminal geometry was measured from 2D screen shots of the rendered images with the foraminal space in-plane with the image. The image shown is for foraminal area measurement.

**Mechanical Testing.** Specimens were positioned by a single laboratory assistant in the neutral position and at the full limits of their ROM in each anatomical direction, e.g., 6 deg of flexion, 3 deg of extension, 10 deg of right and left lateral bending, and 5 deg of axial rotation. For each position, the specimen was held rigidly in place using the halo and rod test setup. The halo neutral position was standardized according to a steinmann pin located through the Frankfurt axis of each specimen as shown in Fig. 1. Each motion was achieved through manipulation of the linear and rotation positioners included on the halo. The amount of rotation or translation of the halo was standardized between the specimens such that the cervical spine relative motion was constant between test series. Once the specimen was positioned, 3D radiographic images were obtained (Philips BV Pulsera 3-D). Flexion, extension, and neutral position specimens were scanned both pre- and post-FJ spacer deployment. Axial rotation and lateral bending specimens were scanned post-FJ spacer deployment only.

**3D Imaging Processing and Analysis.** 3D images were post-processed to quantify changes in foraminal geometry based on guidelines described by Richards et al. [17]. All 3D scans were rendered (Fig. 2, left; Philips BV Pulsera 3D-RX), and screen shots of the rendered images were taken with the foramen of interest being in-plane with the 2D image. These 2D images were then analyzed using commercial code (NIH Image J) to determine the foraminal area. Foraminal area was measured as the total area enclosed by manually identifying boundaries of the foramen using the same reconstructed plane as axial height.

**Outcome Measures and Statistical Analysis.** The increase in foraminal area with insertion of the FJ spacer was the primary outcome measure of interest for foramen testing. Distraction (increase in area) or contraction (decrease in area) of the foramen were measured bilaterally by comparing the dimensions pre and post-FJ spacer deployment for each of the seven motions (neutral, flexion, extension, left/right axial rotation, and left/right lateral bending). Neutral specimens were compared pre- and post- FJ spacer deployment. Flexion, extension, lateral bending, and axial rotation specimens were compared to post-deployment neutral specimens. Distraction/contraction values that were less than 7% were within the bounds of measurement error and were considered to be not significant. A three-part categorical system was used to evaluate the efficacy of the FJ spacer in distracting the foramen as shown in Table 1. Cases with either unilateral or bilateral distraction of the foramen or no distraction or contraction bilaterally

were considered a net increase (“net increase”). Cases with simultaneous distraction on one side and contraction on the other were considered a mixed outcome (“mixed outcome”). Cases exhibiting unilateral or bilateral contraction with no distraction were considered to be net decreases (“net decrease”).

### Methods for Cyclic Fatigue

**Specimen Preparation.** Intact head and neck specimens ( $N = 3$ , cranium-T2, ages 48 to 93, one male, two female) were acquired for both aims of this study with demographics displayed in Table 2. Planar X-ray images were taken prior to deployment of the FJ spacer to exclude specimens with pathological conditions, including pre-existing vertebral fractures, severe osteophyte formation, sagittal plane deformity, or Paget’s disease. Dual X-ray absorptiometry (DEXA) scans were taken of the fatigue group in the AP direction at C1 through C3 (Hologic QDR-2000).

**Table 1 Grading rubric for success or failure of the device during foraminal area testing**

Changes in Area of the Right and Left Foramen	<i>Right no Distraction/Contraction</i>	<i>Right Distraction</i>	<i>Right Contraction</i>
<i>Left no distraction/contraction</i>	net increase	net increase	net decrease
<i>Left distraction</i>	net increase	net increase	mixed outcome
<i>Left contraction</i>	net decrease	mixed outcome	net decrease

**Table 2 Donor information for specimens used throughout this biomechanical study. DEXA scan information is available for specimens 1 through 3 due to the sensitivity of the biomechanical test to BMD**

ID	Level	Age	Sex	C1 DEXA (g/cm <sup>2</sup> )	C2 DEXA (g/cm <sup>2</sup> )	C3 DEXA (g/cm <sup>2</sup> )
1	C4–C5	48	F	0.65	0.77	0.78
1	C6–C7	48	F	0.65	0.77	0.78
2	C4–C5	71	M	0.69	0.8	0.66
2	C6–C7	71	M	0.69	0.8	0.66
3	C4–C5	93	F	0.40	0.52	0.53
3	C6–C7	93	F	0.40	0.52	0.53

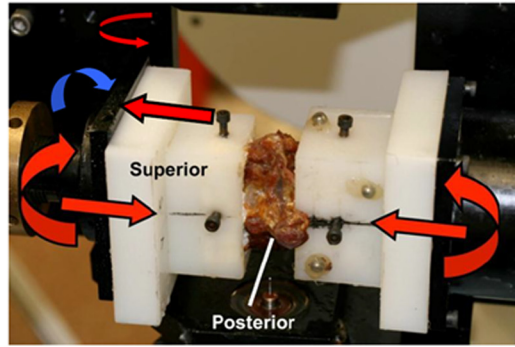
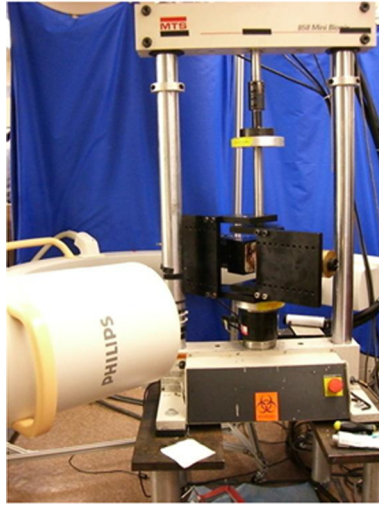


**Fig. 3** (left) The test fixture used for fatigue testing. The c-arm encircled the test fixture. (right) Representative test specimen (09-094 C6–C7) loaded into the fatigue test frame. The red arrows indicate the directions of the applied torque and axial compressive force. The blue arrow shows how the specimen can be rotated to obtain a lateral X-ray image.

DEXA bone mineral density (BMD) scores for these vertebrae were used as a relative measure of bone density across the test population. The FJ spacer was inserted bilaterally at the C4–C5 and C6–C7 levels of each head and neck specimen. The FJ spacer was inserted bilaterally at C4–C5, C5–C6, and C6–C7 levels for the foraminal area group. Insertion was performed with a c-arm available to facilitate and document device positioning. Fatigue specimens were subdivided into C4–C5 and C6–C7 motion segments by careful disarticulation through the C3–C4, C5–C6, and C7–T1 intervertebral disks and facet joints. Specimens were immediately cast in plastic testing cups using a quick-set resin (Smooth Cast 300, Smooth-On, Easton, PA). Vertebrae were potted to maximal depth without interference with articulation of the posterior elements. In some cases, the caudal surface of the inferior spinous process was clipped in order to fit in the casting cups. Specimens were potted such that the geometric center of the disc would be co-linear with the axis of rotation of the testing fixture (Fig. 3, right). Also, proper alignment of the AP and ML directions with the test fixture axes was ensured. Alignment was performed by eye but verified at the time of testing using X-ray. At the time of potting, 2–3 wood screws were inserted into the vertebral endplates and lateral masses of each vertebra to ensure rigid fixation to the potting material. X-ray images were taken prior to casting to ensure that the screws did not interfere with the motion of the disc or posterior elements.

**Mechanical Testing.** Fatigue tests were conducted in angular displacement control between limits corresponding to physiologic bending moments on the cervical spine. This type of testing is similar to the “hybrid protocol” put forth by Panjabi et al. [18] for ROM testing on intact spinal sections, with the exception that the time zero FJ spacer-instrumented functional spinal unit (FSU) was used as the control for imposing the angular limits at >5 K cycle counts. Each FSU was secured to the test fixture in the neutral position and placed under 100 N compressive load [19] via a custom design screw and load cell fixture placed at the cranial and caudal ends of the flexion fixture. A flexion-extension moment of 2.0 Nm was quasi-statically applied, and the corresponding angular displacements were taken as the limits in flexion-extension for the remainder of the fatigue testing. This process was repeated for lateral bending, with the bending limit set at 1.0 Nm. The 2.0 Nm flexion value represents double previously reported values in order to provide a rigorous evaluation of the construct in that direction. The mean flexion/extension ROM at 2.0 Nm was 18.5

+/- 3.5 deg. The mean lateral bending ROM at 1.0 Nm was 5.2 +/- 2.7 deg. This modified hybrid protocol was chosen over purely moment controlled loading because soft-tissue relaxation during long duration fatigue tests can lead to mechanical instability and inadvertent, premature destruction of the specimen. Fatigue tests were conducted at 2 Hz for 30,000 cycles with a 1:1 ratio of flexion-extension to lateral bending loading cycle counts. A compressive load of 100 N was maintained on the specimen throughout testing, and this load was monitored and adjusted for creep at set cycle counts. Testing was interrupted at specified cycle intervals (0, 2500, 5000, 15,000, 30,000) to assess FJ spacer back-out, defined as relative motion between the FJ spacer and the facet joint surfaces. Residual AP (flexion-extension) or ML (lateral bending) moment and axial compressive load were recorded in the neutral position at each of these cycle counts, and compressive load was readjusted to 100 N, if necessary. At 50% of each cycle interval, testing was paused, and the test direction was switched from flexion-extension to lateral bending, or vice versa. For each cycle interval, AP and lateral X-rays were taken with a c-arm positioned around the test frame (see Fig. 4 left; Philips BV Pulsera). The position of the c-arm was locked at the start of the test to allow for a consistent reference frame for all back-out measurements. Specimens were hydrated with a saline solution every 10–15 min throughout testing to minimize tissue decomposition.

**Image Processing and Analysis.** 2D images were post-processed to quantify FJ spacer back-out bilaterally during fatigue testing. Measurements were taken at three of the four corners of each FJ spacer nut using a common reference point as shown in Fig. 5. The reference point for five of six specimens was the tip of a single screw inserted approximately midline into the superior vertebra. Measurements of the screw depth into the vertebra were taken to establish that the screw did not subside during testing. For one specimen, the screw did subside, and a reference point was constructed based on the bony architecture. When visibly evident, back-out of the FJ screw relative to the FJ spacer nut was quantified by measuring the distance between the screw head and a common reference point on the nut.

**Outcome Measures and Statistical Analysis.** The primary outcome measure was FJ spacer back-out defined as the greater of the following two measurements: (1) the relative back-out between the FJ spacer washer along the facet surfaces, and (2) the back-out of the screw within the washer. Clinically significant

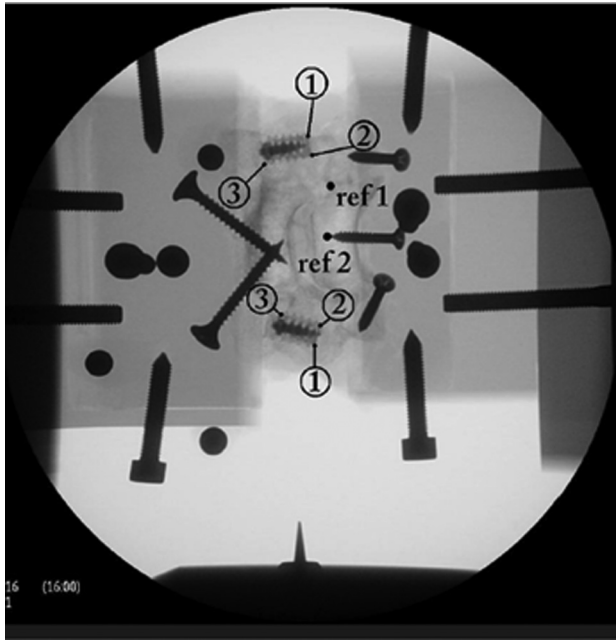


**Fig. 4 Measurement locations 1 through 3 on each device nut. Also shown are the reference points for back-out measurements. Ref 1 is the bony landmark that was used for one specimen, and Ref 2 corresponds to the screw tip that was used in five of six specimens.**

migration of the spacer was determined as the pitch length of the screw 0.5 mm based on the findings of a previous investigation into micromotion [20] that concluded that at 0.5 mm bony ingrowth ceases to progress. As a secondary outcome measure, changes in the bending stiffness of each test specimen were assessed at specific cycle intervals. This information was used to evaluate changes in intervertebral joint mechanics possibly associated with acute device failure, bony fracture, or implant loosening. The moment necessary to impose the fatigue rotation limits was measured for flexion-extension at the 5 K, 10,000, and 22,000 cycle intervals and for lateral bending at 5 K, 5000, and 30,000. Decreases in these moment values correspond to decreased stiffness in a particular loading direction and vice versa.

## Results

Destabilization of the C4/5 motion segment via nucleotomy did not affect ROM in any anatomical direction ( $p > 0.05$  for differences between intact versus destabilized groups) as shown in Fig. 5. Deployment of the FJ spacer as stand-alone decreased relative motion in flexion ( $1.7 \pm 1.5$  times intact values), lateral bending ( $8.4 \pm 7.8$ ), and axial rotation ( $3.9 \pm 2.8$ ); however, there was no significant change versus intact behavior in extension. Addition of an anterior plate decreased motion in extension by a factor of  $5.9 \pm 9.2$ , resulting in a  $6.3 \pm 10$ , a fivefold increase versus intact values. The FJ spacer with anterior plating was significantly more stable than intact and destabilized cases in all loading modes.

In general, a majority of the deployments resulted in successful distraction of the foraminal space as shown in Fig. 6. Foraminal distraction was successful 86% of the time when combining all positions (neutral, flexed, and extended) and all levels (C4–C7). Flexion and extension generated similar successful distraction rates of 83% for both. The success rate for distraction in neutral position was slightly less at 60%. On average, deployment of the FJ spacer in a neutral posture generated an increase of 22%. Extending the specimen generated average distraction of 9%. Of distracted foramen only, the average increase in area was 33% in neutral, 45% in flexed, and 23% in extended postures.

Migration of the FJ spacer was not clinically significant for any FSU specimens as shown in Table 3, and back-out values were less than or equal to 0.5 mm for all devices. All specimens demonstrated some “settling”—generally a substantial decrease in stiffness on the order of 25%–50%—for up to 10,000 cycles, at which point the mechanical response reached a plateau until run-out at 30,000 cycles. There was no indication for any specimen of catastrophic mechanical failure of the device or intervertebral joint, and the gentle decay in stiffness was in line with soft tissue relaxation in the cadaver model.

## Discussion

The FJ spacer system has been evaluated as an effective strategy to stabilize the cervical spine, distract the cervical foramen, and its deployment is robust enough to withstand migration during cyclic loading. We evaluated the biomechanical efficacy of the device in three configurations including multidirection bending motion, dynamic foraminal distraction, and cyclic fatigue. The results of this study indicate that a stand-alone FJ spacer substantially decreased intervertebral motion, remains rigidly engaged in the cervical facet joint space during aggressive bending activity,

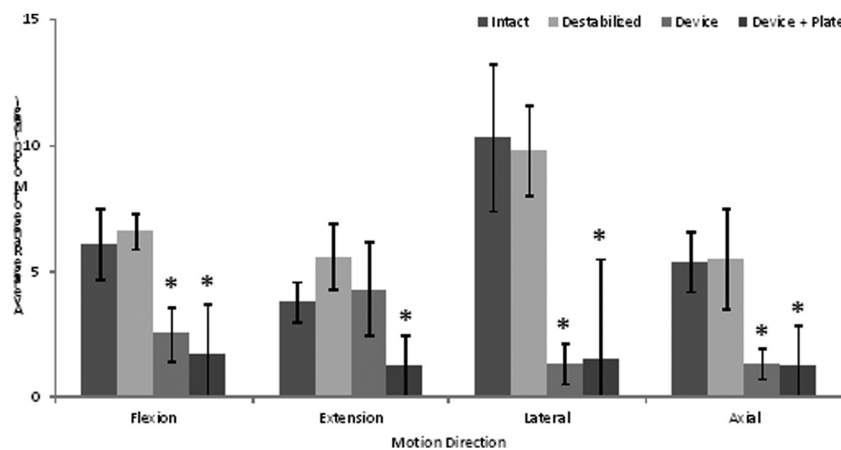


**Fig. 5 Mean multiaxial ROM for intact, destabilized, stand-alone device, and device + plate treatment groups. Error bars represent  $\pm 1$  standard deviation across all samples. (\*)  $p < 0.05$  for difference versus Intact case using repeat measures ANOVA with post hoc adjustment for individual comparisons. Left and right axial rotation and lateral bending have been combined into single mean values as shown.**

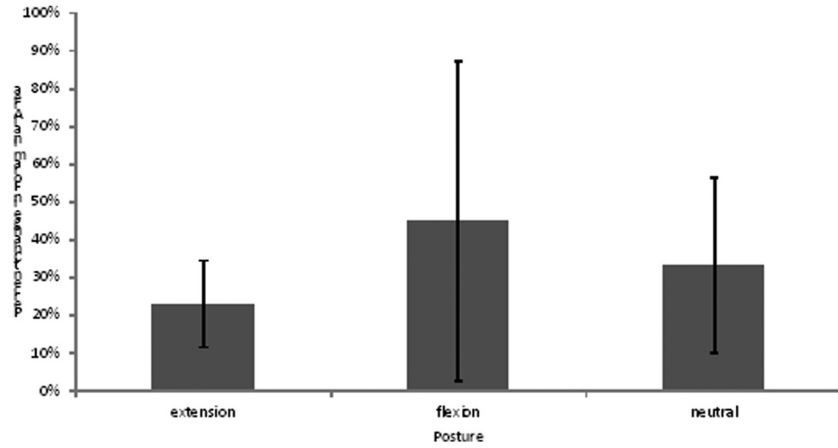


**Fig. 6** Percent increase in foraminal area of distracted specimens only in neutral, flexed, and extended postures. All values represent mean percent change. Error bars represent one standard deviation. Positive values indicate distraction of the foramen. Negative values indicate contraction.

**Table 3** Back-out values and qualitative assessment for all final test specimens. For back-out values, measurement locations are shown in parentheses and correspond to locations provided in Fig. 2. Positive values indicate posterior back-out of the device within the facet, while negative values correspond to anterior back-out.

ID	Level	Left			Back-Out Assessment	Right			Back-Out Assessment
		(1) Back-Out (mm)	(2) Back-Out (mm)	(3) Back-Out (mm)		(1) Back-Out (mm)	(2) Back-Out (mm)	(3) Back-Out (mm)	
1	C4–C5	0.4	0.1	0.5	n.s.	–0.3	–0.4	0.3	n.s.
1	C6–C7	0	–0.3	–0.2	n.s.	–0.1	0.3	0.2	n.s.
2	C4–C5	0.4	0.4	–0.3	n.s.	0	0	0.1	n.s.
2	C6–C7	–0.2	–0.2	–0.4	n.s.	0.1	0	–0.1	n.s.
3	C4–C5	0.1	0	0.2	n.s.	–0.1	–0.1	–0.1	n.s.
3	C6–C7	–0.3	–0.1	0	n.s.	–0.3	–0.4	0	n.s.

and most importantly provides a robust decompression of the cervical nerve root maintained during bending activities.

We observed an insignificant reduction in extension bending with the FJ spacer as stand-alone. We believe this is not due to relative motion of the facets during extension. Instead this is due to compliance of the disc during bending with the FJ spacer transforming the facet joint into a “fulcrum” that may be exploited during quasi-static moment loading configurations that increase the neutral zone and increase total range of motion [21]. The addition of an anterior plate to the FJ spacer constructs provides additional stiffness in extension but does not affect the other bending modes. At any rate, our evidence suggests the neuroforamina remain distracted through extension. Performance of the FJ spacer system investigated in the current study can be compared to two previous quasi-static biomechanical investigations. DalCanto et al. [10] evaluated the stiffness of trans-articular facet fixation with 3.5 mm AO screws. Miyanji et al. [11] evaluated polyaxial screw stiffness (diameter not reported, but assumed to be 3.5 lateral mass screw from DePuy Mountaineer System). Both studies considered fusion constructs at levels between C2/3 and C5/6, and unidirectional bending moments in the range of 1.5 Nm to 2.0 Nm were applied during the testing protocols. The increase in stiffness versus intact for the current FJ spacer was comparable to that demonstrated for 3.5 mm AO screws in flexion, lateral bending, and axial rotation as shown in Fig. 7; however, the increase in stiffness for extension was a factor of 12 less than reported for the AO screws. The ROM in extension in the 3.5 mm AO screw study was unusually low (mean value of 0.5 deg) and comparable to the minimum detectable intervertebral rotation of most experimental set-ups (0.1 deg [22]). Assuming a more conventional value for extension in ROM in a fusion construct (1.0–1.5 deg [23]), the AO screw is likely

2–5 times as stiff as the FJ spacer. Compared to the stand-alone polyaxial screws, the FJ spacer exhibited a greater average increase in stiffness for flexion, lateral bending, and axial rotation.

The FJ spacer system successfully increased the neuroforaminal space in 83% of our observations. We observed the FJ spacer increased foraminal area while the spine was flexed, extended, axially rotated, laterally bent, and in neutral. A majority of the time, the FJ spacer was observed to produce bilateral are increases or unilateral area increases with no adverse effects on the contralateral foramen. Our observation of the absence of area decreases during deployment in a neutral state indicates the FJ spacer is operating as planned on a fundamental level, producing a wedge between the inferior and superior articular processes that translates the facets away from each other producing an increase in neuroforaminal space. Our results during each movement indicate this fundamental mechanism of joint distraction is maintained during physiological motion. Flexion, extension, and axial rotation all produced successful area increases of the foramen at a rate above 75%. These results are not surprising when considering flexion motion where the intended result is distraction of the foramen even in the intact state; however, continued successful increases in area of the foramen during extension (with no decreases observed) corroborates the effect of the FJ spacer’s ability to maintain area increases even in the most demanding environments. Lateral bending produced expected results with a higher success rate in the FJ spacer’s ability to open the foramen contralateral to the direction of the bend. Successful increases in area were also observed in the foramen ipsilateral to the direction of the bend at a rate above 50%. A previous in vitro study [17] investigated the effectiveness of a minimally invasive intraspinal process for lumbar stenosis. The investigators evaluated the

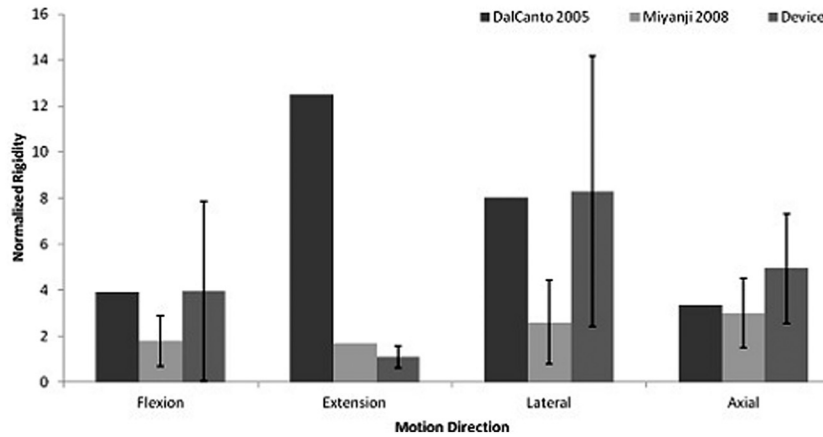


**Fig. 7 Previous studies of stand-alone cervical facet screw fixation versus DTRAX facet screw system stand-alone. Stiffness is normalized to intact values and presented as a multiplier, e.g., 2.5 = “stiffness with implant = 2.5x intact stiffness.” Left and right axial rotation and lateral bending have been combined into single mean values as shown.**

device for increase in area of the foramen in neutral, flexed, and extended postures in a cadaver model. The device generated increases in foraminal area between 20–30%, that is similar to the 24% distraction observed during our investigation. An in vivo investigation into the same lumbar intra-spinous process device [24] measured increases in foraminal area in a small cohort radiographic study. The investigators observed foraminal area increases between 19% to 27%, similar to the results of the device investigate in the current study.

The fatigue loading conditions applied in this protocol are relatively demanding. The cycle count of 30,000 represents two months of bending activity and was derived from a recent kinesiological study by Sterling et al. [25] that monitored head motion during normal activities of daily living in healthy volunteers. From this study, the number of “significant bends”—that is head motion resulting in changes in gaze angle of 90 deg or more—was on the order of 15,000 events monthly. Thus, the 30,000 cycle count used in this protocol represents two months of continuous, aggressive bending activity. Compared to previous in situ fatigue studies involving spinal implants, this study applies one to six times the number of loading cycles [26–32], and we were unable to find any reference to previous experiments in the cervical region that applied more than 6000 loading cycles [28,29]. Furthermore, the applied loading magnitudes for previous cervical fatigue studies have been in the range of 1–1.5 Nm [28,29], that is 25–50% less than the FSU moments applied in this study. In the context of the existing biomechanics literature, this protocol is aggressive in both the number and magnitude of repeated bending cycles. Because of this, we assert that it will provide a conservative—that is to say, worst-case—estimate of the in situ mechanical competence of the device under investigation.

Strengths of our study include a standardized biomechanical evaluation of treatment effects in a repeat-measures design. The results of our study were observed to be comparable to that of predicate devices used for similar indications. This biomechanical model does not take into account biological healing, that may be accelerated in the FJ spacer investigated in this study due to the increased surface area of the device. These claims should be investigated further in animal models and clinical trials. One limitation of our study was a sample size of five (5) for our ROM testing. This sample size is below a minimum expected value; however, the differences we observed in our treatment groups versus intact were clear and statistically significant. We believe this decreased sample size affected the statistical power of our results but did not introduce a type II error. A second limitation of our study is variability in the measurement of foraminal area due to

the multiple grader design of the study. In total, there were 84 3D c-arm scans (two specimens × two FJ spacer deployment states × three levels per specimen × seven anatomical positions) that were analyzed by a team of three researchers. Intrarater variability was quantified by conducting repeated trials of nearly 80% of all foraminal geometry measurements. Variability was assessed to be 7% for all outcome measures. A further limitation of our study was the hybrid method used to fatigue load the specimens. Our method employed a fixed center of rotation that may constrain kinematic motion between the segments. The fixed center of rotation model used may not have permitted relative translations and hence relative sliding motion at the facet. A further limitation of our study was the variability in the measurement of FJ spacer back-out. FJ spacer back-out measurements during fatigue testing were taken by a single, blinded grader using image processing software. Intrarater repeatability for this individual was determined to be 0.25 mm, taken from repeat measurements on a single, randomly selected specimen. The repeatability of the relative migration between the device screw and washer was evaluated by a single, blinded grader and found to be 0.1 mm.

## Acknowledgment

Granting provided by: Providence Medical Inc. (San Francisco CA). Funding and hardware was provided by Providence Medical to perform this study. The authors respectfully acknowledge Mr. Jeffrey Ratusznik MD, Mr. Liu Cheng, and Mr. Chris Han for their support with research and data collection for this study.

## References

- [1] Hughes, J. T., and Brownell, B., 1965, “Necropsy Observations on the Spinal Cord in Cervical Spondylosis,” *Riv. Patol. Nerv. Ment.*, **86**(2), pp. 196–204.
- [2] Irvine, D. H., Foster, J. B., Newell, D. J., and Klukvin, B. N., 1965, “Prevalence of Cervical Spondylosis in a General Practice,” *Lancet*, **22**(1), pp. 1082–1092.
- [3] Pallis, C., Jones, A. M., and Spillane, J. D., 1954, “Cervical Spondylosis; Incidence and Implications,” *Brain*, **77**(2), pp. 274–286.
- [4] Bednarik, J., Kadanka, Z., Dusek, L., Novotny, O., Surelova, D., Urbanek, I., and Prokes, B., 2004, “Presymptomatic Spondylotic Cervical Cord Compression,” *Spine*, **29**(20), pp. 2260–2269.
- [5] Teresi, L. M., Lufkin, R. B., Reicher, M. A., Moffit, B. J., Vinuela, F. V., Wilson, G. M., Benton, J. R., and Hanafee, W. N., 1987, “Asymptomatic Degenerative Disk Disease and Spondylosis of the Cervical Spine: MR Imaging,” *Radiology*, **164**(1), pp. 83–88.
- [6] Tanaka, N., Fujimoto, Y., An, H. S., Ikuta, Y., and Yasuda, M., 2000, “The Anatomic Relation Among the Nerve Roots, Intervertebral Foramina, and Intervertebral Discs of the Cervical Spine,” *Spine*, **25**(3), pp. 286–291.
- [7] Adams, P., and Muri, H., 1976, “Qualitative Changes With Age of Proteoglycans of Human Lumbar Discs,” *Ann. Rheum. Dis.*, **35**(4), pp. 289–296.

- [8] Radhakrishnan, K., Litchy, W. J., O'Fallon, W. M., and Kurland, L. T., 1994, "Epidemiology of Cervical Radiculopathy. A Population-Based Study From Rochester, Minnesota, 1976 Through 1990," *Brain*, (Pt. 2), pp. 325–335.
- [9] Chagas, H., Domingues, F., Aversa, A., Vidal Fonseca, A. L., and de Souza, J. M., 2005, "Cervical Spondylotic Myelopathy: 10 Years of Prospective Outcome Analysis of Anterior Decompression and Fusion," *Surg Neurol.*, (Suppl.), pp. 30–35, discussion S1, pp. 35–36.
- [10] Klekamp, J. W., Uqbo, J. L., Heller, J. G., and Hutton, W. C., 2000, "Cervical Transfacet Versus Lateral Mass Screws: A Biomechanical Comparison," *J. Spinal Disord.*, pp. 515–518.
- [11] Miyanji, F., Mahar, A., Oka, R., and Newton, P., 2008, "Biomechanical Differences Between Transfacet and Lateral Mass Screw-Rod Constructs for Multilevel Posterior Cervical Spine Stabilization," *Spine*, **33**(23), pp. E865–E869.
- [12] DalCanto, R. A., Lieberman, I., Inceoglu, S., Kayanja, M., and Ferrara, L., 2005, "Biomechanical Comparison of Transarticular Facet Screws to Lateral Mass Plates in Two-Level Instrumentations of the Cervical Spine," *Spine*, **30**(8), pp. 897–892.
- [13] Ahmad, F. U., Madhavan, K., Trombly, R., and Levi, A. D., 2012, "Anterior Thigh Compartment Syndrome and Local Myonecrosis After Posterior Spine Surgery on a Jackson Table," *World Neurosurg.*, **78**(5), 553-e5–553-e8.
- [14] Ahn, Y., Lee, S. H., Lee, S. C., Shin, S. W., and Chung, S. E., 2004, "Factors Predicting Excellent Outcome of Percutaneous Cervical Discectomy: Analysis of 111 Consecutive Cases," *Neuroradiology*, **46**(5), pp. 378–384.
- [15] Barnes, A. H., Eguizabal, J. A., Acosta, F. L. Jr., Lotz, J. C., Buckley, J. M., and Ames, C. P., 2009, "Biomechanical Pullout Strength and Stability of the Cervical Artificial Pedicle Screw," *Spine*, **34**(1), pp. E16–E20.
- [16] Acosta, F. L. Jr., Buckley, J. M., Xu, Z., Lotz, J. C., and Ames, C. P., 2008, "Biomechanical Comparison of Three Fixation Techniques for Unstable Thoracolumbar Burst Fractures. Laboratory Investigation," *J. Neurosurg. Spine*, **8**(4), pp. 341–346.
- [17] Richards, J. C., Majumdar, S., Lindsey, D. P., Beaupre, G. S., and Yerby, S. A., 2005, "The Treatment Mechanism of an Interspinous Process Implant for Lumbar Neurogenic Intermittent," *Spine*, **30**(7), pp. 744–749.
- [18] Panjabi, M. M., 2007, "Hybrid Multidirectional Test Method to Evaluate Spinal Adjacent-Level Effects," *Clin. Biomech.*, **22**(3), pp. 257–265.
- [19] Patwardhan, A. G., Havey, R. M., Ghanayem, A. J., Diener, H., Meade, K. P., Dunlap, B., and Hodges, S. D., 2000, "Load-Carrying Capacity of the Human Cervical Spine in Compression Is Increased Under a Follower Load," *Spine*, **25**(12), pp. 1548–1554.
- [20] Overgaard, S., Lind, M., Glerup, H., Bunger, C., and Soballe, K., 1998, "Porous-Coated Versus Grit-Blasted Surface Texture of Hydroxyapatite-Coated Implants During Controlled Micromotion," *J. Arthroplasty*, **13**(4), pp. 449–458.
- [21] Goertzen, D. J., Lane, C., and Oxlund, T. R., 2004, "Neutral Zone and Range of Motion in the Spine Are Greater With Stepwise Loading Than With a Continuous Loading Protocol. An in vitro Porcine Investigation," *J. Biomech.*, **37**(2), pp. 257–261.
- [22] Crawford, N. R., and Dickman, C. A., 1997, "Construction of Local Vertebral Coordinate Systems Using a Digitizing Probe. Technical Note," *Spine*, **1**(1), pp. 559–563.
- [23] Espinoza-Larios, A., Ames, C. P., Chamberlain, R. H., Sonntag, V. K., Dickman, C. A., and Crawford, N. R., 2007, "Biomechanical Comparison of Two-Level Cervical Locking Posterior Screw/Rod and Hook/Rod Techniques," *Spine J.*, **7**(2), pp. 194–204.
- [24] Siddiqui, M., Karadimas, E., Nicol, M., Smith, F. W., and Wardlaw, D., 2006, "Influence of X Stop on Neural Foramina and Spinal Canal Area in Spinal Stenosis," *Spine*, **31**(25), pp. 2958–2962.
- [25] Sterling, A. C., Cobian, D. G., Anderson, P. A., and Heiderscheit, B. C., 2008, "Annual Frequency and Magnitude of Neck Motion in Healthy Individuals," *Spine*, **33**(17), pp. 1882–1888.
- [26] Chiang, C. K., Wang, Y. H., Yang, C. Y., Yang, B. D., and Wang, J. L., 2009, "Prophylactic Vertebroplasty May Reduce the Risk of Adjacent Intact Vertebra From Fatigue Injury: An Ex Vivo Biomechanical Study," *Spine*, **34**(4), pp. 356–364.
- [27] Wang, J. L., Wu, T. K., Lin, T. C., Cheng, C. H., and Huang, S. C., 2008, "Rest Cannot Always Recover the Dynamic Properties of Fatigue-Loaded Intervertebral Disc," *Spine*, **33**(17), pp. 1863–1869.
- [28] Kuroki, H., Rengachary, S. S., Goel, V. K., Holekamp, S. A., Pitkanen, V., and Ebraheim, N. A., 2005, "Biomechanical Comparison of Two Stabilization Techniques of the Atlantoaxial Joints: Transarticular Screw Fixation Versus Screw and Rod Fixation," *Neurosurgery*, **56**(1 Suppl.), pp. 151–159, discussion pp. 151–159.
- [29] Crawford, N. R., Hurlbert, R. J., Choi, W. G., and Dickman, C. A., 1999, "Differential Biomechanical Effects of Injury and Wiring at C1–C2," *Spine*, **24**(18), pp. 1894–1902.
- [30] Zhang, H., Johnston, C. E. 2nd, Pierce, W. A., Ashman, R. B., Bronson, D. G., and Haideri, N. F., 2006, "New Rod-Plate Anterior Instrumentation for Thoracolumbar/Lumbar Scoliosis: Biomechanical Evaluation Compared With Dual-Rod and Single-Rod With Structural Interbody Support," *Spine*, **31**(25), pp. E934–E940.
- [31] Hitchon, P. W., Goel, V. K., Rogge, T. N., Torner, J. C., Dooris, A. P., Drake, J. S., Yang, S. J., and Totoribe, K., 2000, "In Vitro Biomechanical Analysis of Three Anterior Thoracolumbar Implants," *J. Neurosurg.*, **93**(2 Suppl.), pp. 252–258.
- [32] Hitchon, P. W., Goel, V. K., Rogge, T., Grosland, N. M., and Torner, J., 1999, "Biomechanical Studies on Two Anterior Thoracolumbar Implants in Cadaveric Spines," *Spine*, **24**(3), pp. 213–218.